

NG-A50179R; Revised

**The impact of pro-inflammatory cytokines on the  $\beta$ -cell regulatory landscape provides new insights into the genetics of type 1 diabetes**

Ramos-Rodríguez M.<sup>1</sup>, Raurell-Vila H.<sup>1</sup>, Colli ML.<sup>2</sup>, Alvelos MI.<sup>2</sup>, Subirana M.<sup>1</sup>, Juan-Mateu J.<sup>2</sup>, Norris R.<sup>1</sup>, Turatsinze JV.<sup>2</sup>, Nakayasu ES.<sup>3</sup>, Webb-Robertson BJ.<sup>3</sup>, Inshaw JRJ.<sup>4</sup>, Marchetti P.<sup>5</sup>, Piemonti L.<sup>6</sup>, Esteller M.<sup>7,8,9,10</sup>, Todd JA.<sup>4</sup>, Metz TO.<sup>3</sup>, Eizirik DL.<sup>2</sup>, Pasquali L.<sup>1,8,11</sup>

1 Endocrine Regulatory Genomics Laboratory, Germans Trias i Pujol University Hospital and Research Institute, Badalona, Spain.

2 ULB Center for Diabetes Research, Université Libre de Bruxelles, Brussels, Belgium.

3 Biological Sciences Division, Pacific Northwest National Laboratory, Richland, WA, USA.

4 JDRF/Wellcome Diabetes and Inflammation Laboratory, Wellcome Centre for Human Genetics, Nuffield Department of Medicine, NIHR Oxford Biomedical Research Centre, University of Oxford, Roosevelt Drive, Oxford, UK.

5 Department of Clinical and Experimental Medicine, University of Pisa, Pisa, Italy.

6 Diabetes Research Institute (HSR-DRI), San Raffaele Scientific Institute, Milan, 20132, Italy.

7 Cancer Epigenetics and Biology Program (PEBC); Bellvitge Biomedical Biomedical Research Institute (IDIBELL), Barcelona, Catalonia, Spain.

8 Josep Carreras Leukaemia Research Institute (IJC), Badalona, Barcelona, Catalonia, Spain.

9 Institució Catalana de Recerca i Estudis Avançats (ICREA), 08010 Barcelona, Catalonia, Spain.

10 Physiological Sciences Department, School of Medicine and Health Sciences, University of Barcelona (UB), Barcelona, Catalonia, Spain.

11 CIBER de Diabetes y Enfermedades Metabólicas Asociadas (CIBERDEM), Barcelona, Spain.

\*Corresponding author: LP: [lpasquali@igtp.cat](mailto:lpasquali@igtp.cat)

**Abstract:**

Early stages of type 1 diabetes (T1D) are characterized by local autoimmune inflammation and progressive loss of insulin-producing pancreatic  $\beta$  cells. We show here that exposure to pro-inflammatory cytokines unmasks a marked plasticity of the  $\beta$ -cell regulatory landscape. We expand the repertoire of human islet regulatory elements by mapping stimulus-responsive enhancers linked to changes in the  $\beta$ -cell transcriptome, proteome and 3D chromatin structure. Our data indicates that the  $\beta$  cell response to cytokines is mediated by the induction of novel regulatory regions as well as the activation of primed regulatory elements pre-bound by islet-specific transcription factors. We found that T1D-associated loci are enriched of the newly mapped cis-regulatory regions and identify T1D-associated variants disrupting cytokine-responsive enhancer activity in human  $\beta$  cells. Our study illustrates how  $\beta$  cells respond to a pro-inflammatory environment and implicate a role for stimulus-response islet enhancers in T1D.

In type 1 diabetes (T1D), early inflammation of the pancreatic islets (insulitis) by T and B cells contributes to both the primary induction and secondary amplification of the immune assault, with inflammatory mediators such as the cytokines interleukin-1 $\beta$  (IL-1 $\beta$ ) and interferon- $\gamma$  (IFN- $\gamma$ ) contributing to the functional suppression and apoptosis of  $\beta$  cells<sup>1–3</sup>.

Genome wide association studies (GWAS) have made a substantial contribution to the knowledge of T1D genetic architecture uncovering >60 regions containing thousands of associated genetic variants. Nevertheless, translating variants to function remains a main challenge for T1D and other complex diseases. Most of the associated variants do not reside in coding regions<sup>4</sup>, suggesting that they may influence transcript regulation rather than altering protein coding sequences. Recent studies showed a primary enrichment of T1D association signals in T and B cell enhancers<sup>4,5</sup>. A secondary<sup>5</sup>, or a lack of enrichment, was instead observed in islet regulatory regions. While such observation point to a major role of the immune system, we hypothesize that a subset of T1D variants may also act at the  $\beta$ -cell level but only manifest upon islet-cell perturbation and are thus not captured by the current maps of islet regulatory elements.

We have now mapped inflammation-induced *cis*-regulatory networks, transcripts, proteins and 3D chromatin structure changes in human  $\beta$  cells (**Fig. 1a**). We leverage these data to unmask functional T1D genetic variants as well as key candidate genes and regulatory pathways contributing to the  $\beta$  cell autoimmune destruction. Such analyses permit elucidation of the role of epigenetic gene regulation and its interaction with T1D genetics in the context of the autoimmune reaction that drives  $\beta$  cell death.

## Results

***Pro-inflammatory cytokines have a profound impact on the pancreatic  $\beta$ -cell chromatin landscape.*** To characterize the effect of pro-inflammatory cytokines on the  $\beta$ -cell regulatory landscape, we first mapped all accessible or open chromatin sites in human pancreatic islets exposed or not to IFN- $\gamma$  and IL-1 $\beta$ . We assayed chromatin accessibility by ATAC-seq and, in order to focus on the  $\beta$ -cell fraction and to decrease inter-individual variability, in parallel with human pancreatic islet assays, we performed ATAC-seq in the clonal human  $\beta$ -cell line EndoC- $\beta$ H1<sup>6</sup>, exposed or not to the pro-inflammatory cytokines (overall number of peaks identified in human islets: 92,610-229,588; and in EndoC- $\beta$ H1 cells: 52,735-110,715. **Supplementary Fig. 1a**). Such experiments unmasked an important remodeling of the  $\beta$ -cell chromatin resulting in ~12,500 high confident chromatin sites that gain accessibility (FDR adjusted  $P < 0.05$ ;  $|\log_2 FC| > 1$ ) (**Supplementary Fig. 1b**) upon exposure to pro-inflammatory cytokines. Importantly, the changes observed in the human  $\beta$  cell line were concordant with those observed in the human islet preparations (**Supplementary Fig. 1c**).

We reasoned that changes in chromatin accessibility may reflect the activation of non-coding *cis*-regulatory elements. We thus used chromatin immunoprecipitation coupled with next generation sequencing (ChIP-seq) to map cytokine-induced changes of H3K27ac (**Supplementary Fig. 1a**), a key histone modification associated with active *cis*-regulatory elements that was shown to be dynamically regulated in response to acute stimulation<sup>7</sup>. We observed genome-wide deposition of the active histone modification mark upon exposure to pro-inflammatory cytokines in both EndoC- $\beta$ H1 and human pancreatic islets (**Supplementary Fig. 1b-c**).

Integrative analysis of ATAC-seq and ChIP-seq indicates that changes in chromatin accessibility are strongly correlated with deposition of H3K27ac ( $P < 2 \times 10^{-16}$ ,  $r^2 = 0.63$ ) allowing the identification of ~3,800 open chromatin regions that gained H3K27ac (FDR adjusted  $P < 0.05$ ;  $|\log_2 FC| > 1$ ) upon exposure to pro-inflammatory cytokines (**Fig. 1b** and **Supplementary Fig. 1d**). We found that this subset of open chromatin regions is preferentially located distally to gene transcription start sites (TSS) (**Supplementary Fig. 1e**), their sequence is evolutionary conserved (**Supplementary Fig. 1f**) and enriched for specific transcription factor (TF) binding sites (**Supplementary Fig. 1g**). We

named these newly mapped regions IREs for “*Induced Regulatory Elements*” (Supplementary Table 1 and Supplementary Table 2).

**Cytokine-induced regulatory elements drive  $\beta$  cell transcriptomic and proteomic changes.** We next explored whether the newly identified IREs were associated with changes in gene expression and protein translation. To identify  $\beta$  cell transcripts and proteins induced by the pro-inflammatory cytokines we assayed gene expression by RNA-seq (five replicates in EndoC- $\beta$ H1 and five replicates in human pancreatic islets<sup>8</sup>, **Supplementary Fig. 1a**) and collected multiplex proteomics data for three EndoC- $\beta$ H1 replicates after exposure or not to pro-inflammatory cytokines.

In line with the chromatin assays, that indicated extensive gene regulatory activation, we unraveled cytokine-induced transcriptional activation resulting in ~1,200 upregulated genes (FDR adjusted  $P < 0.05$ ;  $|\log_2 FC| > 1$ ) (**Supplementary Fig. 2a-b**). By multiplex proteomics, after rigorous filtering, a subset of 10,166 proteins was confidently quantified and retained for significance testing. A total of 348 proteins displayed significant changes in abundance (FDR/Q-value  $< 0.15$  and  $|FC| > 1.5$ ;  $|\log_2 FC| > 0.58$ ) being 2.19% of the overall detected proteins upregulated (**Supplementary Fig. 2c**), 76% of which had induced mRNA levels at 48h, confirming consistency between RNA-seq and protein changes ( $r^2 = 0.72$ ,  $P < 2 \times 10^{-16}$ ) (**Fig. 1c**). Protein-protein interactions inferred from  $\beta$ -cell cytokine-induced proteins resulted in a network more connected than expected by chance ( $P < 10^{-3}$ ), significantly enriched for Molecular Signatures Database (MSigDB; <http://software.broadinstitute.org/gsea/msigdb/>) pathways including IFN- $\gamma$  signaling, antigen processing and presentation, apoptosis and T1D (KEGG T1D  $P = 7.9 \times 10^{-8}$ , **Supplementary Fig. 2d**).

In line with our expectations we found that IREs were linked to up-regulation of the nearby gene/s as well as to an induced abundance of the corresponding protein (**Fig. 1d-e** and **Supplementary Fig. 2e**). Moreover, gene induction was highly correlated with the number of associated IREs, suggesting a cumulative effect of IREs on cytokine-induced changes in gene expression (**Supplementary Fig. 2f**).

Taken together these findings reveal that pancreatic  $\beta$ -cell response to pro-inflammatory cytokines is dynamic, involving extensive chromatin remodeling and profound changes in the regulatory landscape (**Fig. 1f** and **Supplementary Fig. 2g**). Such changes are associated with induction of transcription and protein translation including pathways implicated in the pathogenesis of T1D. Newly defined regulatory maps can be visualized online (*- upon manuscript publication-*) along with other islet regulatory annotations at [www.isletregulome.org](http://www.isletregulome.org).

***The  $\beta$  cell response to pro-inflammatory cytokines is mediated by primed and neo regulatory elements.*** We next sought to gain insight into the dynamic activation of IREs. The relationship between chromatin openness and H3K27ac deposition upon exposure to pro-inflammatory cytokines allows the distinction of two classes of IREs (**Fig. 1b** and **Fig. 2a-c**): “*opening IREs*” ( $n=2,436$ ) which gain both chromatin accessibility ( $\log_2 \text{FC} > 1$ ) and H3K27ac ( $\log_2 \text{FC} > 1$ ); and “*primed IREs*” ( $n=1,362$ ) which are already accessible chromatin sites prior to the treatment (ATAC-seq  $\log_2 \text{FC} < 1$ ) and gain H3K27ac ( $\log_2 \text{FC} > 1$ ) upon exposure to the stimulus. Primed and opening IREs are both associated to gene expression induction (**Supplementary Fig. 3a**), phylogenetically conserved (**Supplementary Fig. 3b**) and preferentially mapped distally relatively to gene TSS (**Supplementary Fig. 3c**). We further unmasked that 70% of opening IREs ( $n=1,716$ ) are regions of complete novel activation (i.e. undetectable in basal condition, see methods). We named the latter “*neo IREs*”. Neo IREs represent 45% of all IREs and may mirror “*latent enhancers*” that were identified upon stimulation of mouse macrophages<sup>7</sup>.

Because chromatin openness, the feature discerning the two classes of IREs, is believed to reflect TF occupancy, we analyzed their sequence composition in search of recognition sequences of key TFs orchestrating the  $\beta$  cell response to pro-inflammatory cytokines. Even though IREs are mostly distal to TSS (**Supplementary Fig. 3c**), in order to reduce sequence biases, we excluded from this analysis all annotated promoters. The two classes of distal IREs predominantly mapped to enhancer chromatin state (**Supplementary Fig. 3d**) and showed clear differences in sequence composition. Newly induced enhancers were enriched for binding motifs of inflammatory-response TFs

including Interferon-Sensitive Response Element (ISRE), STAT and NF- $\kappa$ B (**Supplementary Fig. 3e**). Primed enhancers instead were enriched for binding motifs of inflammatory-response TFs (ISRE, STAT), and unexpectedly, islet-specific TFs (HNF1A/B, NEUROD1, PDX1, MAFB, NKX6.1) (**Supplementary Fig. 3f**). Importantly, we found that, in primed enhancers, inflammatory-response and islet-specific TFs binding motifs mapped to the same genomic region, suggesting co-binding and possibly cooperation of the two classes of TFs (**Supplementary Fig. 3g-h**).

Sequence composition bias *per se* does not imply TF occupancy. We thus took advantage of published ChIP-seq datasets of islet-specific TFs (MAFB, PDX1, FOXA2, NKX6.1 and NKX2.2) mapped in un-stimulated human pancreatic islets<sup>9</sup> to measure TF occupancy in primed and neo enhancers prior to the pro-inflammatory stimulus. As expected from the sequence composition analysis, primed enhancers (unlike neo enhancers) are highly bound by tissue-specific TFs even before their activation (**Fig. 2d** and **Supplementary Fig. 3i**). TF occupancy can also be indirectly assessed by ATAC-seq, which assays the protection of the bound sequence to transposase cleavage (footprint). Footprint analysis is effective for TFs with a long residence time<sup>10</sup> such as IRFs and STAT TF families. Our analyses revealed the emergence of footprint marks upon pro-inflammatory treatment in correspondence to ISRE motifs in both primed and neo enhancers (**Fig. 2e**) indicating cytokine-induced TF occupancy of IREs.

Gene regulation is orchestrated by different epigenetics mechanisms. DNA methylation is a relatively stable epigenetic mark contributing to maintenance of cellular identity<sup>11,12</sup>. Moreover, high-resolution DNA methylation maps, obtained from multiple tissues, established that the vast majority of tissue-specific differentially methylated regions are located at distal, mostly non-coding, regulatory sites<sup>13</sup>. Consequently, characterization of the DNA methylome in the context of relevant stimuli is important for understanding the functional mechanisms of tissue-specific responses in human disease<sup>14</sup>. We thus explored if cytokine-induced chromatin remodeling is associated with changes in DNA methylation. We quantified DNA methylation changes by performing dense methylation arrays in EndoC- $\beta$ H1 exposed or not to IFN- $\gamma$  and IL-1 $\beta$ . The Infinium MethylationEPIC array was designed to interrogate with

high precision and coverage >850,000 CpG sites (approximately 3% of all sites in the genome) selected primarily because of their location close to gene promoters and CpG-island regions. By focusing on the 1,230 IRE enhancers harboring one or more CpG sites interrogated by the array, we observed that primed enhancers overlap lowly methylated CpGs (median  $\beta$ -value  $0.12 \pm 0.08$ ), that did not vary significantly upon cytokine exposure. Such observation is in sharp contrast with neo enhancers that were highly methylated under control condition (median  $\beta$ -value  $0.77 \pm 0.10$ ) but underwent a significant loss of DNA methylation (Wilcoxon test,  $P = 4.13 \times 10^{-4}$ ) upon the treatment (**Fig. 2f**). While we did not observe cytokine-induced methylation, we found that ~70% of the significantly demethylated probes (FDR adjusted  $P \leq 0.05$ ;  $\beta_{\text{cyt}} - \beta_{\text{ctrl}} < -0.20$ ) mapping to IRE were located at neo enhancers (**Supplementary Fig. 3j,k**)

These results suggest that neo enhancers are enriched for methylated CpGs that undergo preferential demethylation upon cytokine treatment whereas primed enhancers are enriched for unmethylated CpGs that do not change their methylation status upon the cytokine exposure.

Taken together these analyses lead to a model, in which pro-inflammatory cytokines elicit a regulatory response in  $\beta$  cells characterized by: 1) induction of novel distal regulatory elements coupled with reduction of DNA methylation and binding of inflammatory response TFs and 2) activation of regulatory elements pre-bound by islet-specific TFs and induced by inflammatory response TFs (**Fig. 2g**).

Collectively, these results allow reconstructing *cis*-regulatory networks activated in human pancreatic  $\beta$  cells upon exposure to the pro-inflammatory cytokines IFN- $\gamma$  and IL-1 $\beta$  (**Supplementary Fig. 4a-c** and **Supplementary Table 1**).

**Activation of regulatory elements is coupled with changes in the 3D chromatin structure.** Regulatory regions can exert control over genes at megabase distances through the formation of DNA loops. These loops are often confined within structures known as topologically associating domains (TADs)<sup>15–17</sup>. TADs are largely conserved upon evolution, are invariant in different cell types and have their boundaries defined by the regulatory scope of tissue-specific enhancers<sup>18–20</sup>. Our knowledge regarding the general



characteristics and mechanisms of loops is improving<sup>21–24</sup>, but much less is known regarding mechanisms and functional significance of dynamic looping events during biological processes.

We took advantage of promoter capture Hi-C (pcHi-C) performed in human pancreatic islets<sup>25</sup> to explore long-range interactions between gene promoters and cytokine-induced and invariant distant regulatory elements. Interestingly, we observed that the interaction confidence scores captured between IRE enhancers and gene promoters in untreated islets were significantly reduced compared with SREs enhancers ( $P=1.8\times 10^{-11}$ ) (**Supplementary Fig. 5a**). As this finding point to potential dynamic properties of the interaction maps, we next sought to investigate if cytokine-induced regulatory changes are linked to modification of the 3D chromatin structure and if induction of  $\beta$ -cell cytokine-responsive regulatory elements is coupled with the formation of novel DNA looping interactions.

Hi-C profiles are limited in sequencing coverage and library complexity, resulting in maps of reduced resolution relative to regulatory maps of functional elements. On the other hand, 4C approaches are difficult to interpret quantitatively mainly due to potential amplification biases. We thus applied targeted chromosome capture with unique molecular identifiers (UMI-4C), a recently developed method<sup>26</sup>, to quantitatively measure interaction intensities in human islets before and after exposure to pro-inflammatory cytokines. We centered the conformation capture viewpoint to the promoter of 13 genes (*TNFSF10*, *GBP1*, *CIITA*, among others) whose expression was strongly induced by the cytokine exposure.

UMI-4C showed marked changes in the 3D chromatin structure at the analyzed loci. Promoters of the induced genes gained chromatin interactions with distal genomic regions reflecting the formation of new DNA looping events (**Fig. 3a-b** and **Supplementary Fig. 5b-d**). Importantly, such new contacts were preferentially engaged with newly mapped human islet cytokine-responsive IREs (**Fig. 3c**).

These results demonstrate that cytokine exposure induces changes in human islet 3D chromatin conformation including the formation of novel enhancer-promoter interactions. Such changes allow the newly activated distal IREs to contact their target gene promoters.

**Cytokine induced islet regulatory elements are implicated in T1D genetic susceptibility.** GWAS have identified ~60 chromosome regions associated with T1D<sup>27</sup> with many of the association signals having been assigned to candidate genes with immunological functions. Consistent with this notion, several studies reported a primary enrichment of T1D risk variants in T and B cell regulatory elements<sup>4,5</sup>. Furthermore, there is a substantial lack of statistical significant overlap of T1D associated variants in islet enhancers, while such regulatory elements are instead enriched for GWAS signals for T2D and fasting glucose<sup>9,28</sup>. Nonetheless, the molecular mechanisms linking T1D association signals to cellular functions remain poorly described for most of the regions of association identified.

We hypothesized that a subset of T1D genetic signals may reflect an altered capacity of the  $\beta$  cells to react to an inflammatory environment. We thus sought to explore to what extent genetic signals underlying T1D susceptibility act through pancreatic islet regulatory response to pro-inflammatory cytokines.

Causal *cis* variants are expected to lie in sequences that act as regulatory regions in state-specific and disease-relevant tissues. We thus examined non shared loci with genome-wide significant association to T2D and T1D in European populations and considered all variants in high LD (1000 Genomes Project phase3 EUR  $R^2 > 0.8$ ) with a lead SNP reported in the NHGRI-EBI GWAS catalog<sup>29</sup>. In line with previous observations<sup>4,9</sup>, we found that T2D but not T1D risk variants overlap human islet non cytokine-responsive regulatory elements (i.e. SREs) more than expected by chance (T2D SNPs in SREs  $P < 2 \times 10^{-16}$ ,  $Z = 5.47$ ). In contrast, we uncovered that human islet IREs are enriched for T1D but not T2D risk variants (T1D SNPs in IREs  $P = 3 \times 10^{-6}$ ,  $Z = 4.61$ ) (**Fig. 4a**). This result was reproduced when using regulatory elements detected in EndoC- $\beta$ H1 cells (**Supplementary Fig. 6a**). Such findings unmasked 15 T1D associated regions (21% of the total) containing at least one IRE and putative target genes whose expression was cytokine-responsive. In 8 of these regions, the IREs directly overlap a T1D associated variant (**Supplementary Table 3**). All of these regions have the potential to harbor functional *cis*-regulatory variants, opening an avenue to the identification of T1D candidate genes acting at the  $\beta$ -cell level (**Supplementary Fig. 6b-f**).

We noticed that the two T1D lead SNPs at 1q24.3 and 16q13.13 loci (rs78037977<sup>30</sup> and rs193778<sup>4</sup> respectively) were directly overlapping IREs in islets. We used GWAS genotyping data from a cohort of 14,575 individuals (5,909 T1D cases and 8,721 controls, see methods) to confirm their association with T1D. Both variants were included in the 99% credible set of their respective locus and displayed strong association *P*-values (rs78037977  $P=6.94e^{-10}$ ; rs193778  $P=1.33e^{-7}$ ; see **Supplementary Table 4** for posterior probability of association and variant ranking in the credible set), indicating that they could potentially be causal.

At the 1q24.3 locus, rs78037977 overlaps an islet cytokine-induced chromatin site (**Fig. 4b**) which is pre-bound by islet-specific TFs and is a predicted enhancer in other cell types (**Supplementary Fig. 6g**). We created allele-specific luciferase reporter constructs and measured enhancer activity in the EndoC- $\beta$ H1 line before and after cytokine exposure. The sequence exerts enhancer activity exclusively after cytokine exposure which is disrupted by the rs78037977, T1D associated, G allele (**Fig. 4c** and **Supplementary Fig. 6h**) consistent with a causal role of the variant at this locus. In order to identify the gene target of this T1D-susceptible enhancer, we reconstructed the 3D chromatin structure by chromatin capture experiments. UMI-4C in human islets identified a cytokine-induced interaction of the enhancer with *TNFSF18* a gene activated in islets upon cytokine exposure (**Fig. 4d-e**). *TNFSF18* encodes for a cytokine, ligand of the TNFRSF18/GITR receptor, known to modulate inflammatory reaction and regulation of autoimmune responses<sup>31</sup>. Interestingly, we noticed that cytokine exposure results in upregulation of *TNFSF18* in human islets but not in the EndoC- $\beta$ H1  $\beta$ -cell line, suggesting differences in gene regulatory dynamics in primary tissue or the activation of an islet cell sub-population.

At the 16q13.13 locus, rs193778 maps to a phylogenetically conserved, cytokine-responsive regulatory element (**Fig. 4f**). This sequence displays enhancer activity in both treated and untreated  $\beta$  cells. However, exclusively in cytokine-exposed  $\beta$  cells, the T1D-associated G allele exerts significantly higher enhancer activity than the protective variant (**Fig. 4g** and **Supplementary Fig. 6i**). The locus includes several up-regulated genes (*SOCS1*, *DEXI*, *CIITA*, *RM12*), that could represent potential targets of this IRE. Recent works point to

*DEXI* as a T1D candidate gene in immune cells and  $\beta$  cells<sup>32,33</sup>. By performing UMI-4C experiments in human islets we observed a strong chromatin contact between the promoter of *DEXI* and the regulatory element bearing the rs193778 T1D-associated variant (**Fig. 4h**). Such data points to *DEXI* as a potential causal gene in pancreatic islets.

Altogether these results illustrate how unraveling cytokine-induced chromatin dynamics in human islets can guide the identification of *cis*-regulatory variants that are strong candidates in driving T1D-association signals.

## Discussion:

Our work illustrates the human pancreatic  $\beta$  cell chromatin dynamics in response to an external stimulus that may be relevant in the context of T1D. We here show that exposure to pro-inflammatory cytokines causes profound remodeling of the  $\beta$ -cell regulatory landscape coupled with changes in gene expression and protein production. We unveil the activation of ~3,600 cytokine-responsive distal *cis* regulatory elements and reveal a lack of homogeneity in their molecular mechanism of activation. We observed that the induction of a subset of novel regulatory regions (neo IREs) require TF binding and chromatin opening while other chromatin sites are “primed” to their activation being pre-bound by islet-specific TFs. Our observations suggest a model in which binding of tissue-specific TFs may facilitate chromatin accessibility at a subset of chromatin sites that can then be promptly activated by the induction of inflammatory-response TFs. Such model is supported by very recent findings<sup>34</sup> and consistent with observations in murine macrophages<sup>7,35</sup> and murine dendritic cells<sup>36</sup>, but thus far had not been demonstrated in a highly differentiated and non-immune related tissue such as the pancreatic islets.

Importantly, we show that such regulatory changes are coupled with 3D chromatin remodeling, allowing the newly activated regulatory elements to contact their target genes. Several reports described 3D chromatin dynamics properties in the cell developmental context<sup>37,38</sup>, upon loss of cell fate<sup>39,40</sup>, senescence<sup>41,42</sup> or in response to hormonal exposure<sup>43</sup>. Our observations indicate that the capacity of enhancer loop formation is maintained in a highly-differentiated tissue such as the islets and it is coupled with transcriptional regulatory changes, in response to an external stimulus.

The model used in our study to explore chromatin dynamics is of particular interest because it mimics the inflammatory environment that the pancreatic islets may face in the early stages of T1D. While several T1D candidate genes regulating key steps related to “danger signal recognition” and innate immunity were shown to be expressed in human islets<sup>44</sup>, T1D associated variants were shown to be enriched for immune cell types but not in stable pancreatic islets regulatory elements<sup>4</sup>. Such apparent contradiction may be reconciled by our findings showing that human islet cytokine-responsive regulatory elements are enriched for T1D risk variants. Our data, supported by recent findings unmasking regulatory variants affecting enhancer activation in immune response<sup>34,45</sup>, opens the avenue to identify T1D molecular mechanisms acting at the pancreatic islet cells level.

Although we cannot exclude that functional variants disrupting  $\beta$ -cell regulatory mechanisms may at the same time affect the regulatory potential of immune-related cell types, the availability of stimulus-responsive cis-regulatory maps in pancreatic islets will facilitate hypothesis-driven experiments to uncover how common and lower frequency genetic variants impact islet cells in T1D. We here studied the human islet responses to a specific pro-inflammatory stimulus. Future work, studying additional immune-mediated stresses potentially affecting  $\beta$  cells at different stages of the disease, may allow uncovering other association signals acting at the islet cell level.

In general, our findings could apply by extension to other diseases where “primed” enhancers may facilitate cell-type-specific responses to ubiquitous signals resulting in tissue-specific genetic susceptibility in autoimmune diseases.

#### **Acknowledgments:**

This work by LP was supported by grants from the Spanish Ministry of Economy and Competitiveness (BFU2014-58150-R and SAF2017-86242-R to LP), Marató TV3 (201624.10, to LP) and a young investigator award from the Spanish Society of Diabetes to LP. The Pasquali lab is further supported by ISCIII (PIE16/00011). LP is a recipient of a Ramon y Cajal contract from the Spanish Ministry of Economy and Competitiveness (RYC-2013-12864) and MR is supported by an FI Agència de Gestió d'Ajuts Universitaris i de Recerca

(AGAUR) PhD fellowship. JJ was supported by a MSCA fellowship grant from the Horizons 2020 EU program (Project reference: 660449). Human islets were provided through the European Consortium for Islet Transplantation (ECIT) distribution program for basic research supported by JDRF award 31-2008-416. DLE was supported by grants from the Fonds National de la Recherche Scientifique (FNRS), Welbio CR-2015A-06, Belgium; the Horizon 2020 Program, T2Dsystems (GA667191); Brussels Capital Region-Innoviris (project Diatype), and the Innovative Medicines Initiative 2 Joint Undertaking under grant agreement No 115797 (INNODIA). This Joint Undertaking receives support from the Union's Horizon 2020 research and innovation programme and "EFPIA", "JDRF" and "The Leona M. and Harry B. Helmsley Charitable Trust. TOM and DLE were supported by a grant of the National Institutes of Health, NIH-NIDDK-HIRN Consortium 1UC4DK104166-01. Part of the work was performed in the Environmental Molecular Sciences Laboratory, a U.S. Department of Energy (DOE) national scientific user facility at Pacific Northwest National Laboratory (PNNL) in Richland, WA. Battelle operates PNNL for the DOE under contract DE-AC05-76RLO01830. We thank Josep Mercader and Marta Guindo Martínez for helpful discussions regarding GWAS enrichment analyses.

#### **Author contributions:**

L.P., M.R. and D.L.E. designed the experiments. H.R., M.C., M.A., J.J., R.N. and E.N. performed and analyzed the experiments. M.R. performed bioinformatic analyses with contribution from M.S., J.T., B.W. and J.I.. L.Pi., P.M., M.E., and T.M. provided material and resources. L.P., D.L.E., T.M. and J.T. supervised the study. LP and MR coordinated, conceived the project and wrote the manuscript with contribution from D.L.E. All authors reviewed the final manuscript.

#### **Declaration of interests**

Authors declare no conflict of interest.

#### **Data availability:**

Datasets for induced regulatory elements (IREs) in both EndoC- $\beta$ H1 and human pancreatic islets are available upon request and will be available for download and visualization upon publication at the Islet Regulome Browser<sup>46</sup> ([www.isletregulome.com](http://www.isletregulome.com)).

Raw sequencing reads for the different assays (RNA-seq, proteomics, ATAC-seq, ChIP-seq, UMI-4C) will be made available at GEO.

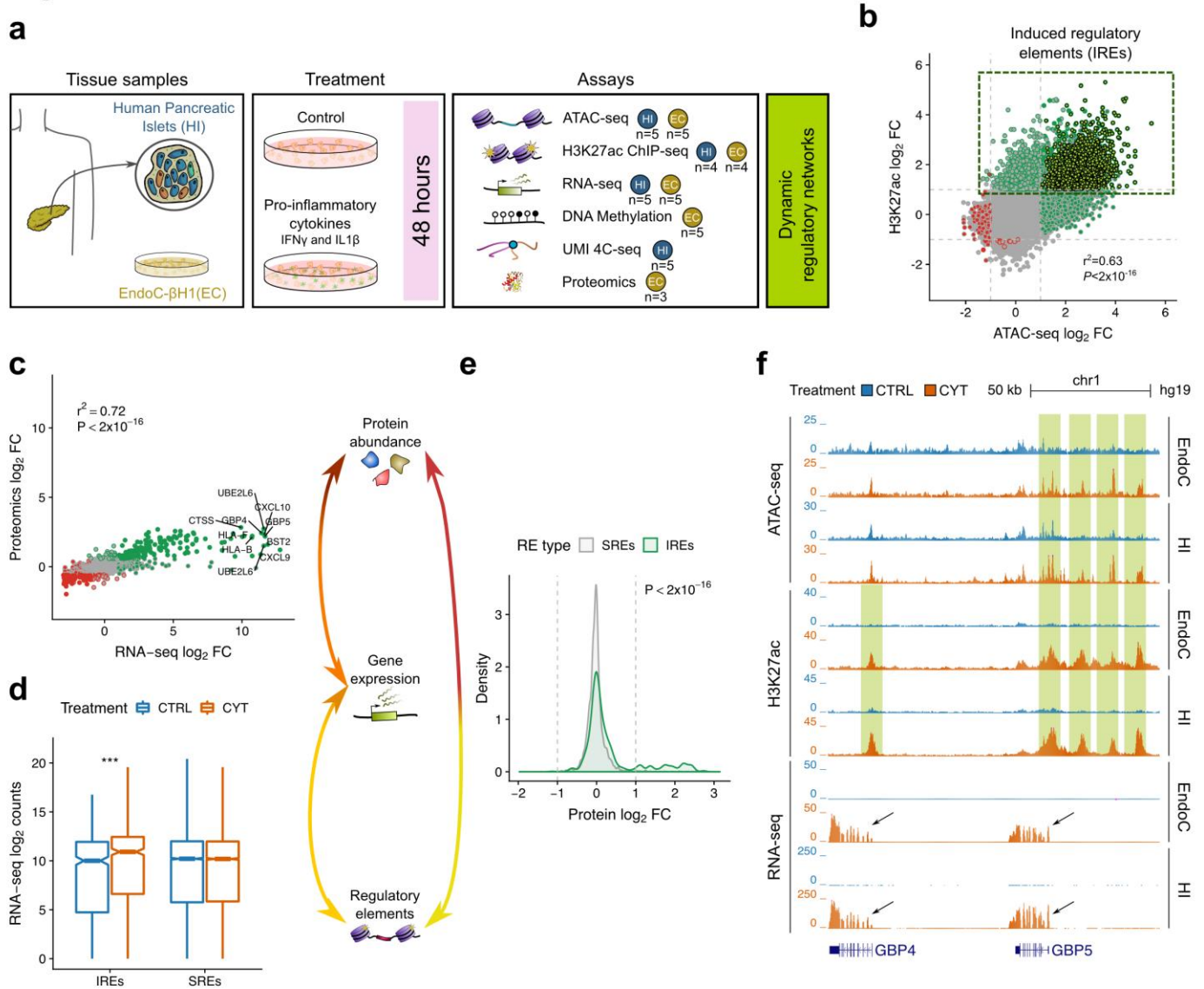
## References:

1. Todd, J. A. Etiology of Type 1 Diabetes. *Immunity* **32**, 457–467 (2010).
2. Ziegler, A.-G. & Nepom, G. T. Prediction and Pathogenesis in Type 1 Diabetes. *Immunity* **32**, 468–478 (2010).
3. Eizirik, D. L., Colli, M. L. & Ortis, F. The role of inflammation in insulinitis and beta-cell loss in type 1 diabetes. *Nat. Rev. Endocrinol.* **5**, 219–26 (2009).
4. Onengut-Gumuscu, S. *et al.* Fine mapping of type 1 diabetes susceptibility loci and evidence for colocalization of causal variants with lymphoid gene enhancers. *Nat. Genet.* **47**, 381–386 (2015).
5. Farh, K. K. *et al.* Genetic and Epigenetic Fine-Mapping of Causal Autoimmune Disease Variants. *Nature* **518**, 337–343 (2015).
6. Ravassard, P. *et al.* A genetically engineered human pancreatic  $\beta$  cell line exhibiting glucose-inducible insulin secretion. *J. Clin. Invest.* **121**, 3589–3597 (2011).
7. Ostuni, R. *et al.* Latent Enhancers Activated by Stimulation in Differentiated Cells. *Cell* **152**, 157–171 (2013).
8. Gonzalez-Duque, S. *et al.* Conventional and Neo-Antigenic Peptides Presented by  $\beta$  Cells Are Targeted by Circulating Naïve CD8+ T Cells in Type 1 Diabetic and Healthy Donors. *Cell Metab.* (2018). doi:10.1016/j.cmet.2018.07.007
9. Pasquali, L. *et al.* Pancreatic islet enhancer clusters enriched in type 2 diabetes risk-associated variants. *Nat. Genet.* **46**, 136–143 (2014).
10. Sung, M.-H., Guertin, M. J., Baek, S. & Hager, G. L. DNase Footprint Signatures Are Dictated by Factor Dynamics and DNA Sequence. *Mol. Cell* **56**, 275–285 (2014).
11. Bird, A. DNA methylation patterns and epigenetic memory. *Genes Dev.* **16**, 6–21 (2002).
12. Hemberger, M., Dean, W. & Reik, W. Epigenetic dynamics of stem cells and cell lineage commitment: digging Waddington's canal. *Nat. Rev. Mol. Cell Biol.* **10**, 526–537 (2009).
13. Lister, R. *et al.* Human DNA methylomes at base resolution show widespread epigenomic differences. *Nature* **462**, 315–322 (2009).
14. Feinberg, A. P. Phenotypic plasticity and the epigenetics of human disease. *Nature* **447**, 433–440 (2007).
15. Dixon, J. R. *et al.* Topological domains in mammalian genomes identified by analysis of chromatin interactions. *Nature* **485**, 376–380 (2012).
16. Nora, E. P. *et al.* Spatial partitioning of the regulatory landscape of the X-inactivation centre. *Nature* **485**, 381–385 (2012).
17. Dekker, J., Marti-Renom, M. A. & Mirny, L. A. Exploring the three-

- dimensional organization of genomes: interpreting chromatin interaction data. *Nat. Rev. Genet.* **14**, 390–403 (2013).
18. Symmons, O. *et al.* Functional and topological characteristics of mammalian regulatory domains. *Genome Res.* **24**, 390–400 (2014).
  19. Krivega, I., Dale, R. K. & Dean, A. Role of LDB1 in the transition from chromatin looping to transcription activation. *Genes Dev.* **28**, 1278–1290 (2014).
  20. Lee, J. *et al.* Chromatin remodeller Fun30Fft3 induces nucleosome disassembly to facilitate RNA polymerase II elongation. *Nat. Commun.* **8**, 14527 (2017).
  21. Yu, M. & Ren, B. The Three-Dimensional Organization of Mammalian Genomes. *Annu. Rev. Cell Dev. Biol.* **33**, 265–289 (2017).
  22. Rowley, M. J. & Corces, V. G. Organizational principles of 3D genome architecture. *Nat. Rev. Genet.* **19**, 789–800 (2018).
  23. Schoenfelder, S. & Fraser, P. Long-range enhancer–promoter contacts in gene expression control. *Nat. Rev. Genet.* **1** (2019). doi:10.1038/s41576-019-0128-0
  24. Stadhouders, R., Filion, G. J. & Graf, T. Transcription factors and 3D genome conformation in cell-fate decisions. *Nature* **569**, 345–354 (2019).
  25. Miguel-Escalada, I. *et al.* Human pancreatic islet 3D chromatin architecture provides insights into the genetics of type 2 diabetes. *bioRxiv* (2018). doi:10.1101/400291
  26. Schwartzman, O. *et al.* UMI-4C for quantitative and targeted chromosomal contact profiling. *Nat. Methods* **13**, 685–691 (2016).
  27. Todd, J., Burren, O., Schofield, E., Carver, T. & Achuthn Premanand. ImmunoBase. Available at: <https://www.immunobase.org/>. (Accessed: 20th May 2019)
  28. Parker, S. C. J. *et al.* Chromatin stretch enhancer states drive cell-specific gene regulation and harbor human disease risk variants. *Proc. Natl. Acad. Sci.* **110**, 17921–17926 (2013).
  29. MacArthur, J. *et al.* The new NHGRI-EBI Catalog of published genome-wide association studies (GWAS Catalog). *Nucleic Acids Res.* **45**, D896–D901 (2017).
  30. Cooper, N. J. *et al.* Type 1 diabetes genome-wide association analysis with imputation identifies five new risk regions. *bioRxiv* 120022 (2017). doi:10.1101/120022
  31. Ray, A., Basu, S., Williams, C. B., Salzman, N. H. & Dittel, B. N. A Novel IL-10-Independent Regulatory Role for B Cells in Suppressing Autoimmunity by Maintenance of Regulatory T Cells via GITR Ligand. *J. Immunol.* **188**, 3188–3198 (2012).
  32. Davison, L. J. *et al.* Long-range DNA looping and gene expression analyses identify DEXI as an autoimmune disease candidate gene. *Hum. Mol. Genet.* **21**, 322–333 (2012).
  33. Dos Santos, R. S. *et al.* DEXI, a candidate gene for type 1 diabetes, modulates rat and human pancreatic beta cell inflammation via regulation of the type I IFN/STAT signalling pathway. *Diabetologia* **62**, 459–472 (2019).
  34. Alasoo, K. *et al.* Shared genetic effects on chromatin and gene expression indicate a role for enhancer priming in immune response. *Nat. Genet.* **50**, 424–431 (2018).



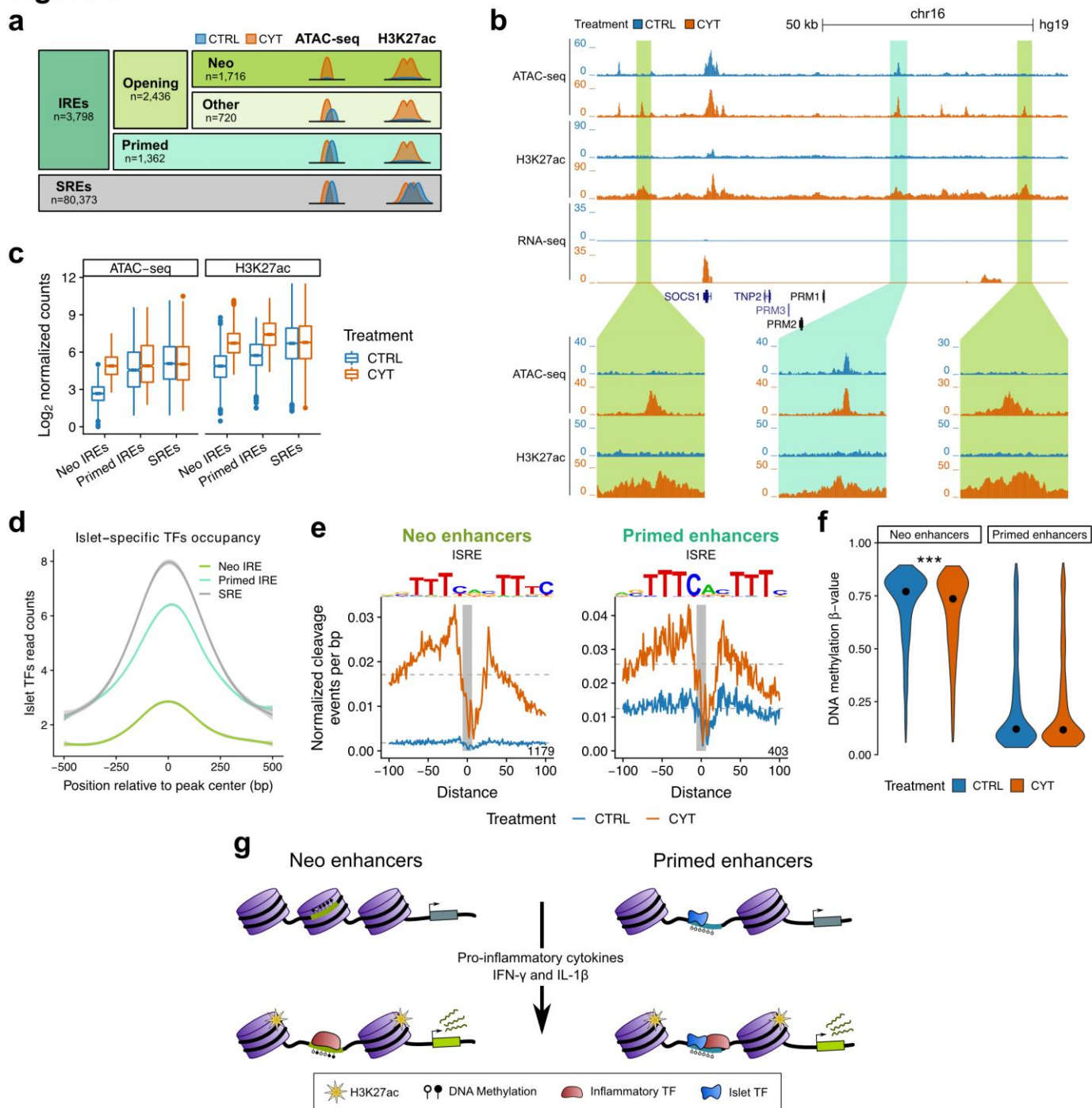
35. Heinz, S. *et al.* Effect of natural genetic variation on enhancer selection and function. *Nature* **503**, 487–492 (2013).
36. Vandenbon, A., Kumagai, Y., Lin, M., Suzuki, Y. & Nakai, K. Waves of chromatin modifications in mouse dendritic cells in response to LPS stimulation. *Genome Biol.* **19**, 138 (2018).
37. Phanstiel, D. H. *et al.* Static and Dynamic DNA Loops form AP-1-Bound Activation Hubs during Macrophage Development. *Mol. Cell* **67**, 1037–1048.e6 (2017).
38. Mumbach, M. R. *et al.* Enhancer connectome in primary human cells identifies target genes of disease-associated DNA elements. *Nat. Genet.* **49**, 1602–1612 (2017).
39. Taberlay, P. C. *et al.* Three-dimensional disorganization of the cancer genome occurs coincident with long-range genetic and epigenetic alterations. *Genome Res.* **26**, 719–731 (2016).
40. Barutcu, A. R. *et al.* Chromatin interaction analysis reveals changes in small chromosome and telomere clustering between epithelial and breast cancer cells. *Genome Biol.* **16**, 214 (2015).
41. Chandra, T. *et al.* Global Reorganization of the Nuclear Landscape in Senescent Cells. *Cell Rep.* **10**, 471–483 (2015).
42. Criscione, S. W. *et al.* Reorganization of chromosome architecture in replicative cellular senescence. *Sci. Adv.* **2**, e1500882 (2016).
43. Le Dily, F. *et al.* Distinct structural transitions of chromatin topological domains correlate with coordinated hormone-induced gene regulation. *Genes Dev.* **28**, 2151–2162 (2014).
44. Op de Beeck, A. & Eizirik, D. L. Viral infections in type 1 diabetes mellitus — why the  $\beta$  cells? *Nat. Rev. Endocrinol.* **12**, 263–273 (2016).
45. Kim-Hellmuth, S. *et al.* Genetic regulatory effects modified by immune activation contribute to autoimmune disease associations. *Nat. Commun.* **8**, 266 (2017).
46. Mularoni, L., Ramos-Rodríguez, M. & Pasquali, L. The pancreatic islet regulome browser. *Front. Genet.* **8**, 1–8 (2017).

**Figure 1**

**Figure 1. Pro-inflammatory cytokines exposure causes profound remodeling of the human pancreatic  $\beta$ -cells regulatory landscape.**

**a**, Summary of the experimental design. Multi-omics experiments were performed upon exposure or not of human pancreatic islets and EndoC- $\beta$ H1 cells to IFN- $\gamma$  and IL-1 $\beta$  to reconstruct cytokine-responsive dynamic regulatory networks. The number of human pancreatic islets (HI) and EndoC- $\beta$ H1 (EC) independent samples used in different assays is indicated at the side of each assay schematic representation. **b**, Correlation between chromatin accessibility and H3K27ac deposition. Each dot corresponds to a chromatin site, the x-axis indicating the ATAC-seq signal  $\log_2$  FC and y-axis the  $\log_2$  FC of the H3K27ac ChIP-seq signal. Point fill refers to the ATAC-seq and the border to the H3K27ac classification (gained=green; lost=red; stable=grey). The dotted box depicts the regulatory elements referred as induced regulatory elements (IREs) and the lighter shade of green depicts a subtype of these, named neo IREs (see text). **c**, Correlation between

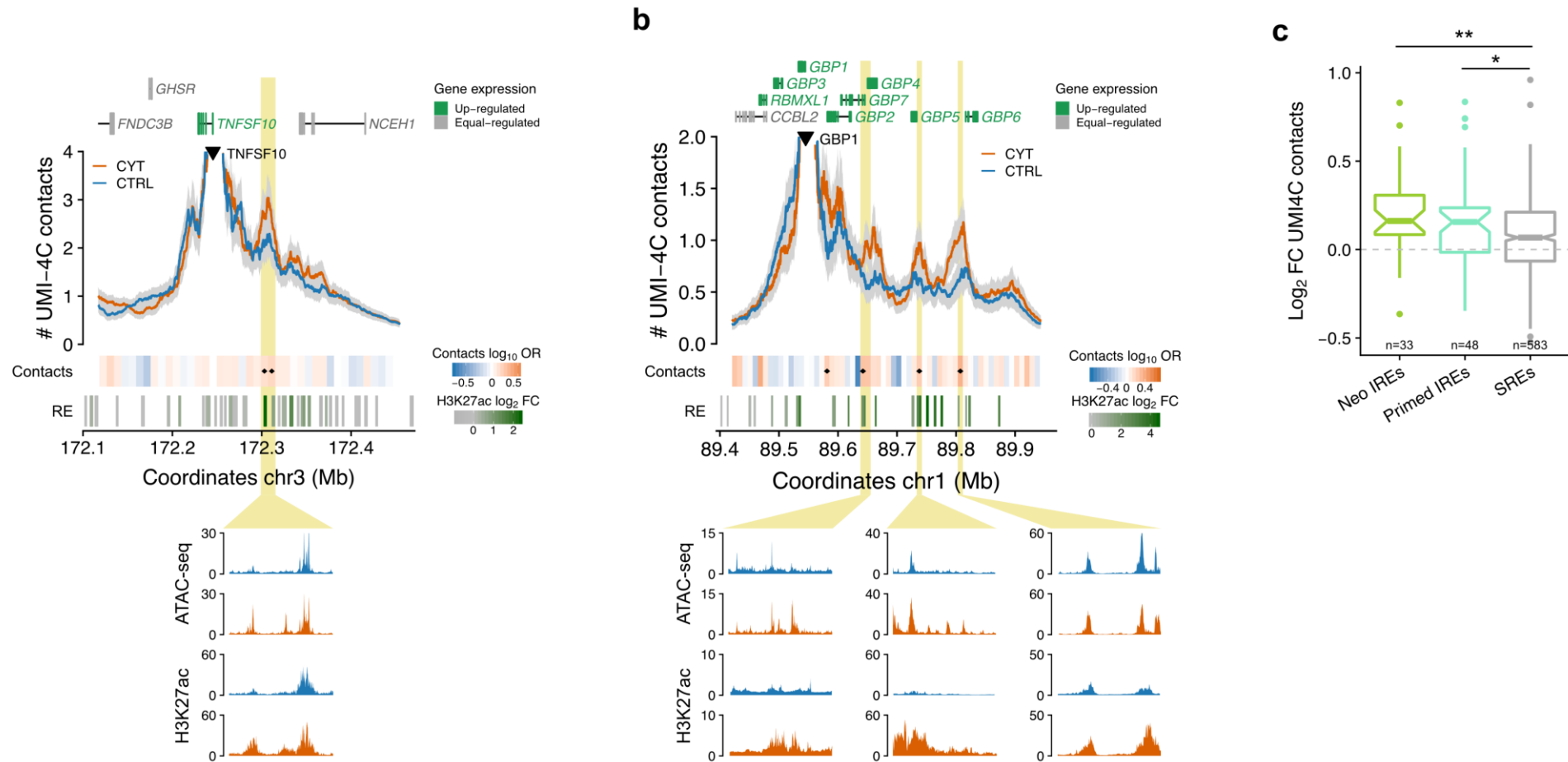
changes in RNA expression and the corresponding protein abundance. The x-axis shows the  $\log_2$  FC for the RNA expression and the y-axis the  $\log_2$  FC for the protein abundance (both in EndoC- $\beta$ H1 cells). Point fill indicates the RNA-seq classification and the border indicates the protein classification (up-regulated=green; down-regulated=red; equal-regulated=grey). **d**, Genes located <15 kb from IREs show cytokine-induced expression in EndoC- $\beta$ H1 cells exposed or not to pro-inflammatory treatment. CYT= cytokine exposed (orange), CTRL = not exposed to cytokine (blue). \*\*\* Wilcoxon test  $P < 0.001$ . Box plot limits show upper and lower quartiles, whiskers extend to 1.5 times the interquartile range. **e**, Abundance of proteins encoded by IRE-associated genes is induced by cytokine exposure in EndoC- $\beta$ H1 cells. This is shown by the significantly different (Wilcoxon test  $P < 2 \times 10^{-16}$ )  $\log_2$  FC distribution of protein abundance obtained after exposure or not of EndoC- $\beta$ H1 to IFN- $\gamma$  and IL-1 $\beta$  (n=3), for proteins encoded by genes located <15 kb from IREs or stable regulatory elements (SREs). **f**, Representative view of the IFN-inducible guanylate binding proteins *GBP4* and *GBP5*, showing the up-regulation of these genes upon cytokine exposure and the nearby induction of IREs characterized by gains in chromatin accessibility and enrichment in H3K27ac (green boxes).

**Figure 2**

**Figure 2. The  $\beta$  cell response to pro-inflammatory cytokine unveils neo and primed regulatory elements.**

**a**, Classification of ATAC-seq open chromatin sites upon exposure of human  $\beta$  cells to IFN- $\gamma$  and IL-1 $\beta$ . IREs=induced regulatory elements, SREs=stable regulatory elements. **b**, View of the *SOCS1* locus, a gene strongly induced upon pro-inflammatory cytokine exposure. We here depict representative examples of primed (blue box) and neo IREs (green boxes). **c**, Box plot distribution of ATAC-seq and H3K27ac normalized tag counts at different classes of IREs. Box plot limits show upper and lower quartiles, whiskers extend to 1.5 times the interquartile range, individual

data points represent outliers and the notch represents the confidence interval around the median. **d**, Islet-specific TF occupancy at neo, primed and stable regulatory elements. Read density for PDX1, NKX2.2, FOXA2, NKX6.1 and MAFB was calculated in 10bp bins in 1kb windows centered on the regulatory element. Lines represent means, while the grey shade depicts standard deviations. **e**, Footprint analysis of ISRE motifs in neo (left) and primed regulatory elements (right) in cells exposed or not to IFN- $\gamma$  and IL-1 $\beta$  (control = blue; cytokines = orange). **f**, Violin plots showing the distribution of DNA methylation  $\beta$ -values in neo and primed enhancers, exposed or not to pro-inflammatory cytokines. \*\*\* Wilcoxon test  $P < 0.001$ . **g**, Model showing two types of IREs driving the response to pro-inflammatory cytokines in human  $\beta$  cells.

**Figure 3****Figure 3. Cytokine exposure induces changes in human islet 3D chromatin structure.**

**a, b**, View of the UMI-4C chromatin contacts of *TNFSF10* (**a**) and *GBP1* (**b**) promoters, before and after exposure to pro-inflammatory cytokines. Yellow boxes indicate IREs that gain contacts with the up-regulated gene promoters. A heatmap under the 4C track represents the log<sub>10</sub> odds ratio (OR) of the UMI-4C contacts difference in cytokine vs. control. Small black diamonds on top of the contact heatmap indicate a significant

difference between cytokine-treated and control samples 3D chromatin contacts (Chi-squared  $P < 0.05$ ). ATAC-seq peaks are represented by rectangles shaded from gray to green proportionally to the cytokine-induced H2K27ac  $\log_2$  fold change observed at that site (RE=regulatory elements track). **c**, Distribution of the UMI-4C contacts  $\log_2$  fold changes (cytokines vs. control) at the different types of islets open chromatin sites classified as in **Fig. 2a**. The data, obtained by analyzing viewpoints centered at the promoter of cytokine-induced genes, show that the chromatin structural changes are preferentially happening at IREs. Box plot limits show upper and lower quartiles, whiskers extend to 1.5 times the interquartile range, individual data points represent outliers and the notch represents the confidence interval around the median.

**Figure 4**

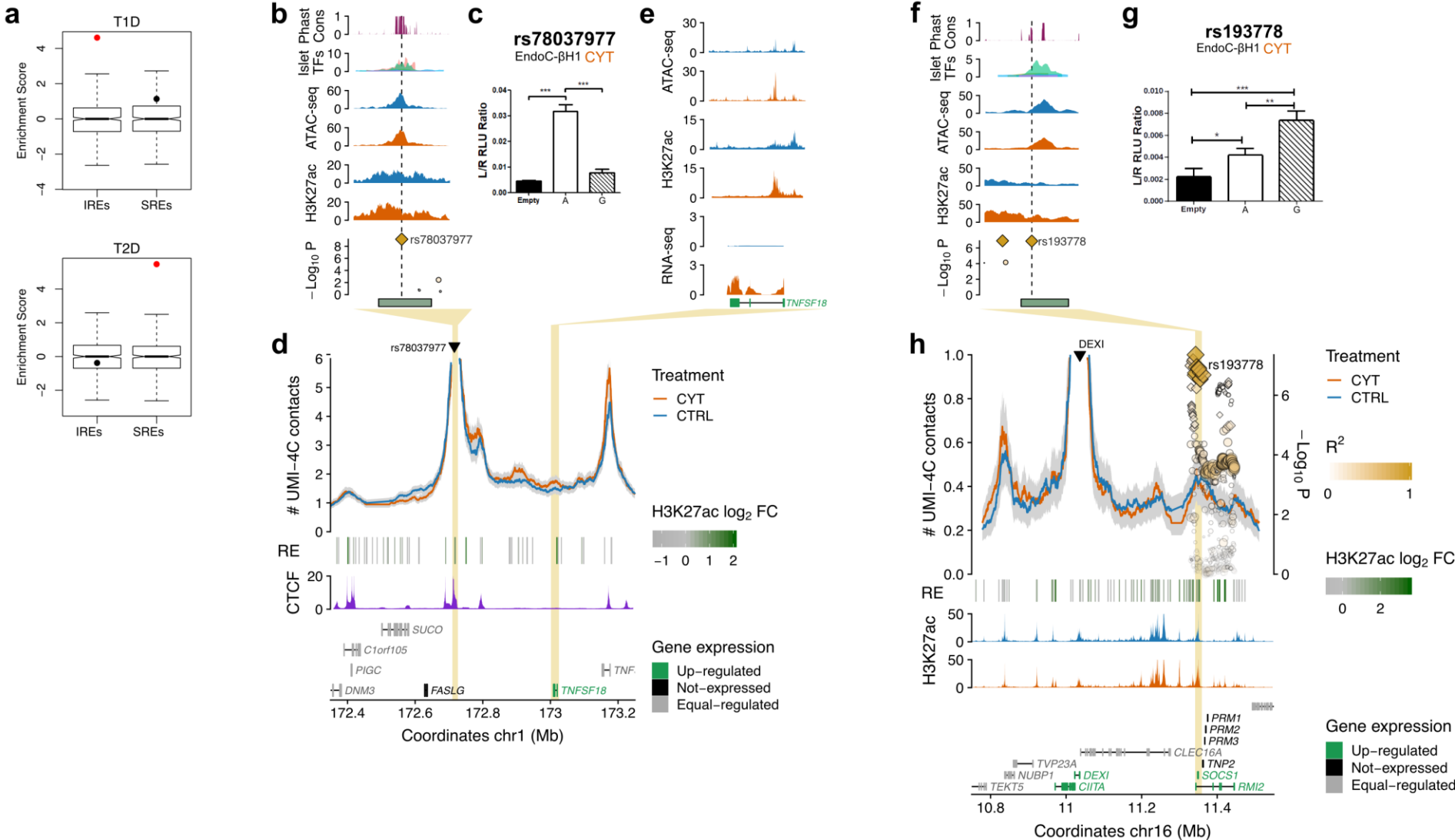


**Figure 4. Cytokine-induced islet regulatory elements map to T1D associated regions and guide the identification of functional risk variants.**



**a**, Human islet induced regulatory elements (IREs) are enriched for T1D but not T2D risk variants. In contrast, human islet stable regulatory elements (SREs) overlap, more than expected by chance, T2D but not T1D risk variants. Each dot denotes the Variance Set Enrichment (VSE) score in IREs or SREs regions. Significant enrichments over the null distribution are depicted in red (Bonferroni adjusted  $P < 0.05$ ). The box plots illustrate the enrichment distribution of matched null sets based on 500 permutations. Box plot limits show upper and lower quartiles, whiskers extend to 1.5 times the interquartile range and the notch represents the confidence interval around the median. **b**, rs78037977 is the highest associated variant in the 1q24.3 T1D associated locus. The variant overlaps an IRE bound by islet-specific TFs under basal conditions. **c**, Luciferase assays in EndoC- $\beta$ H1 exposed to pro-inflammatory cytokines show that, in these conditions, the sequence exerts enhancer activity which is reduced in the T1D associated allele (G) compared to the non-risk allele (A). **d**, UMI-4C analysis performed in human islets show that the cytokine-responsive regulatory element containing rs78037977 engages multiple distal chromatin contacts, some of which are induced upon INF- $\gamma$  and IL-1 $\beta$  treatment and others coinciding with CTCFs binding sites. **e**, Zoom-in view at one induced chromatin contact, mapping to an IRE in proximity of the up-regulated *TNFSF18* gene, a potential target of the IRE containing rs78037977 T1D functional variant. **f**, Variant rs193778 is part of the 99% credible set driving the association with T1D at the 16q13.13 locus and maps to a phylogenetically conserved IRE. **g**, Luciferase assays for the underlying sequence performed in EndoC- $\beta$ H1 exposed to INF- $\gamma$  and IL-1 $\beta$  show significantly increased enhancer activity of the risk (G) allele compared to the non-risk (A) allele. **h**, UMI-4C analysis performed in pancreatic islets using the promoter of *DEXI* as viewpoint, show a chromatin contact with the IRE bearing the T1D variant. ATAC-seq peaks are represented, in **d** and **h**, by rectangles shaded from gray to green proportionally to the cytokine-induced H2K27ac  $\log_2$  fold change observed at that site (RE=regulatory elements track).